

Utility of real-time field control in T_2^* imaging at 7T

Yolanda Duerst¹, Michael Wyss¹, Bertram J Wilm¹, Benjamin E Dietrich¹, Simon Gross¹, David O Brunner¹, Thomas Schmid¹, and Klaas P Pruessmann¹
¹ETH Zurich, Zurich, ZH, Switzerland

INTRODUCTION – T_2^* -weighted gradient echo imaging is particularly sensitive to field distortions due to the required long echo times. Respiratory motion of the chest causes time-varying changes in the magnetic susceptibility distribution and thereby gives rise to dynamic field perturbations [1]. The effect scales with the main magnetic field strength and has been reported to cause artifacts in T_2^* -weighted imaging at 7T [2,3]. To address this problem, real-time higher order field control has recently been proposed [4] to correct for field changes and hence related image artifacts without the need to change pulse sequences or image reconstruction. The present work aims to assess the practical utility of this approach. To this end it studies the degree of breathing perturbations in dependence on body mass index (BMI), the related artifacts, and the capability of field control to mitigate them.

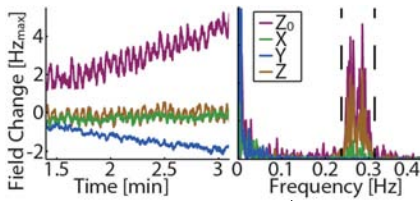


Fig. 1: Sample time series of 0^{th} and 1^{st} order spherical harmonics (left). Fourier transform of the data and filter bounds (right).

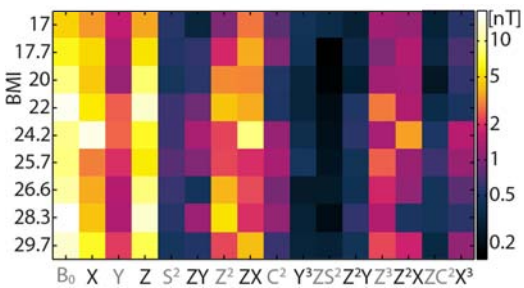


Fig. 2: Standard deviation of 0^{th} to 3^{rd} order spherical harmonics terms in the frequency range associated with breathing. The volunteers are sorted according to their body mass index (BMI). Cosine (C) and sine (S) terms can be expressed by X and Y according to $C^2 = X^2 - Y^2$, $S^2 = XY$.

the exception of one volunteer (BMI: 22) which was suspected to have moved his head during the examination. As might be expected for breathing induced field changes, the main contributions were in B_0 , Z (fh), and X (ap), while in the Y (lr) direction much less breathing related oscillations were observed. Furthermore, terms with no or little dependence on Z and X (as for example Y^2 or ZS^2) showed little variation in all volunteers. The interpolated field changes in the slices (Fig. 3) showed a decrease in standard deviation with increasing distance from the chest. The data also reconfirm the increase in fluctuations with increasing BMI.

Statistic over all volunteers shows that artifact magnitude was reduced by real-time field control in all three sectors and for all types of artifact (Fig. 4). Artifact types that showed strong effects (e.g. ghosting or ringing) were diminished, however not removed completely. Weaker artifacts on the other hand (e.g. signal loss and intensity modulations) were fully corrected in most cases. Without feedback field control an average of 8.8 out of 20 slices per subject suffered from disturbing artifacts (2 or higher), where in 8 out of 9 volunteers one or more slices were disturbed. By using real-time feedback this was reduced to an average of 2.9 out of 20 slices that were disturbed, affecting 5 out of 9 volunteers.

Two example images without and with feedback are shown in Fig. 5. Without real-time feedback ghosting, signal loss, and ringing artifacts were observed which could be removed when turning on field stabilization.

CONCLUSION – Field fluctuations due to breathing manifested mostly in 0^{th} and 1^{st} order spherical harmonics, but also in a few 2^{nd} and 3^{rd} order terms. As expected for field changes that arise due to chest motion, field fluctuations decreased with increasing distance from the source and were generally stronger for volunteers with higher BMI. The application of full 3^{rd} order real-time feedback achieved effective field stabilization and strongly reduced the artifact level in the images.

Stable field evolution in 16 probes with feedback control (data not shown) indicates that remaining image artifacts are not due to limited feedback bandwidth but rather caused by incomplete modeling of the field fluctuations by 3^{rd} order spherical harmonics. An increased number of field probes and shim terms, as well as tailored shim field patterns may be explored for further improved correction of breathing induced field changes.

REFERENCES – [1] Van de Moortele et al., MRM 2002;47:888-895 [2] Versluis et al., NeuroImage 2010;51:1082-1088 [3] Van Gelderen et al., MRM 2007;57:362-368 [4] Duerst et al., Proc. ISMRM 2013;p.669 [5] Barmet et al., MRM 2008;60:187-197

METHODS – T_2^* -weighted gradient echo scans of the head were acquired in transverse orientation (FOV: 240x190 mm², TR: 1000 ms, TE: 25 ms, in-plane resolution: 0.3 mm, slice thickness: 1.5 mm, 20 slices) in 9 healthy subjects (BMI: 17.0 – 29.7, 4 males). Each volunteer was scanned once without field feedback and once with feedback. All measurements were performed on a whole-body 7T Philips Achieva system (Philips Healthcare, Cleveland, USA).

The real-time field feedback system consisted of 16 NMR field probes [5] to measure field changes every 50 ms. A proportional-integral controller was used to calculate shim updates to minimize deviations from the targeted uniform field configuration. The updated shim demands were subsequently fed to the gradient and shim amplifiers [4].

In order to quantify the magnitude of breathing induced field changes, measured field deviations were decomposed into 0^{th} to 3^{rd} order spherical harmonics. These signals were filtered with a band pass over the frequency range corresponding to respiration which was determined for each subject individually. The standard deviation of the resulting oscillations was then calculated for each spherical harmonic term. Furthermore, the spherical harmonics in the respiratory frequency range were used to interpolate the field patterns at the locations of the imaged slices. For each volunteer the standard deviation of the field change in each voxel was calculated and averaged over the slice.

Image artifacts were classified into 5 different groups: ghosting, signal loss, ringing, intensity modulation, and blurring. In each slice the artifacts were rated individually for their severity according to 0: nonexistent, 1: slightly visible, 2: disturbing, 3: strong. The rating was then averaged within three segments: below the third ventricle (S1), between the third and the lateral ventricles (S2), and above the lateral ventricles (S3).

RESULTS – Standard deviations of 0^{th} to 3^{rd} order spherical harmonics (Fig. 2) showed a clear increase in fluctuations in B_0 and Z with increasing BMI of the volunteer, with the

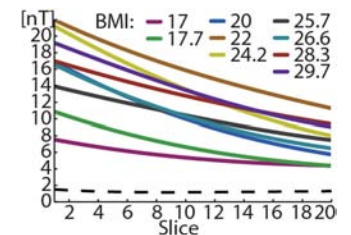


Fig. 3: Standard deviation of the field changes due to breathing at the position of the imaged slices for 9 volunteers. The dashed line indicates intrinsic field stability.

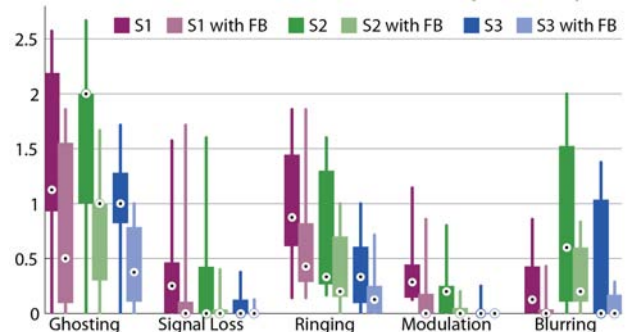


Fig. 4: Magnitude of the individual artifacts in the three sectors (S1 to S3), each with (light color) and without (full color) feedback. The dots indicate the median over the 9 volunteers, the boxes range from the 25. to 75. percentile, the lines reach to the maximum and minimum values.

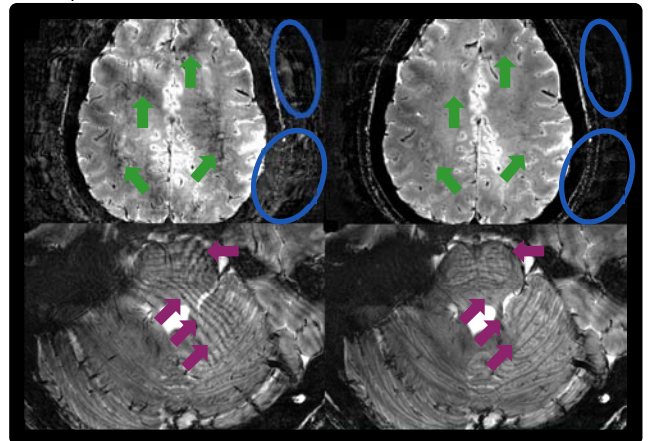


Fig. 5: Example of signal loss (green), ghosting (blue), and ringing (red) artifacts without (left) and with (right) real-time field control.